Superconductor Science and Technology

PAPER • OPEN ACCESS

A new ductile, tougher resin for impregnation of superconducting magnets

To cite this article: Emanuela Barzi *et al* 2024 *Supercond. Sci. Technol.* **37** 045008

OPEN ACCESS
IOP Publishing

Superconductor Science and Technology

Supercond. Sci. Technol. **37** (2024) 045008 (10pp)

https://doi.org/10.1088/1361-6668/ad2c25

A new ductile, tougher resin for impregnation of superconducting magnets

Emanuela Barzi[1,6,*], Daniele Turrioni[1], Ibrahim Kesgin[2], Masaki Takeuchi[3], Wang Xudong[4], Tatsushi Nakamoto[4] and Akihiro Kikuchi[5]

[1] Fermi National Accelerator Laboratory, Batavia, IL 60510, United States of America
[2] Argonne National Laboratory, Lemont, IL 60439, United States of America
[3] RIMTEC Corporation, Kurashiki-shi, Okayama 711-0934, Japan
[4] High Energy Accelerator Research Organization (KEK), Tsukuba, Ibaraki 305-0801, Japan
[5] National Institute for Materials Science, Tsukuba, Ibaraki 305-0047, Japan
[6] Ohio State University, Columbus, OH 43210, United States of America

E-mail: barzi@fnal.gov

Received 6 November 2023, revised 15 January 2024
Accepted for publication 22 February 2024
Published 7 March 2024

Abstract

A major remaining challenge for Nb_3Sn high field magnets is their training due to random temperature variations in the coils. The main objective of our research is to reduce or eliminate it by finding novel impregnation materials in replacement of the epoxies currently used. An organic olefin-based thermosetting dicyclopentadiene resin, $C_{10}H_{12}$, commercially available in Japan as TELENE® by RIMTEC, was used to impregnate a short Nb_3Sn undulator coil developed by ANL and FNAL. This magnet reached short sample limit after only two quenches, compared with ∼100 when CTD-101K® was used. Ductility, i.e. the ability to accept large strains, and toughness were identified as key properties to achieve these results. In addition, we have been investigating whether mixing TELENE with high heat capacity ceramic powders such as Gd_2O_3, Gd_2O_2S, and $HoCu_2$, increases the specific heat (C_p) of impregnated Nb_3Sn superconducting magnets. The viscosity, heat capacity, thermal conductivity, and other physical properties of TELENE with high-C_p powder fillers were measured in this study as a function of temperature and magnetic field. The TELENE-87 wt%Gd_2O_2S had a peak in C_p between 4.3 K and 5.3 K at fields between 0 and 8 T. We have also investigated the effect on the mechanical properties of pure and mixed TELENE under 10 MGy of gamma ray irradiation at the Takasaki Advanced Radiation Research Institute in Takasaki, Japan. TELENE-87 wt%Gd_2O_2S exhibited exceptional radiation resistance. Impregnating an undulator coil with TELENE mixed with Gd_2O_2S powder will verify whether the coils' thermal stability further improves, or whether its low diffusivity will require engineering the material with high-thermal conductivity components. Short magnet training will lead to better magnet reliability, lower magnet margins, lower risk and substantial saving in accelerators' commissioning costs. Part of this study is

* Author to whom any correspondence should be addressed.

supported by the U.S.-Japan Science and Technology Cooperation Program in high energy physics operated by MEXT in Japan and DOE in the U.S.

Keywords: superconducting magnet, training, dicyclopentadiene, resin impregnation, specific heat

1. Introduction

One of the main challenges of Nb_3Sn high field accelerator magnets for high energy physics is their training [1]. Superconducting (SC) magnets go back to being resistive from their SC state, i.e. 'quench', when their temperature increases above the current sharing temperature of the composite superconductor over a large enough volume. The temperature increase ΔT is proportional to Q/C_p, where Q is the dissipated heat, and C_p is the volumetric heat capacity. Energy deposition that initiates quenches can emanate from a variety of both mechanical and electromagnetic sources (magnetic flux jumps, conductor motion, epoxy cracking, etc). Other sources of magnet training are material interfaces, such as between conductor, insulation, impregnating material, and neighboring structural materials. All these sources contribute to a resulting 'disturbance spectrum'.

Long training has been a feature of any Nb_3Sn impregnated magnet for decades, since the start of the development of this technology. Any attempt made so far to reduce magnet training with materials and methods applicable to accelerator magnets failed. We show here almost total training elimination when using as coil impregnation material for a Nb_3Sn magnet $C_{10}H_{12}$, an organic olefin-based thermosetting dicyclopentadiene (DCP) resin, in replacement of the CTD-101K® epoxy currently used for this purpose. This resin is commercially available as TELENE® by RIMTEC Corporation, Japan, and its molecular structure and molecular formula are shown in figure 1. It was used to impregnate an ANL Nb_3Sn short undulator model, which at every training cycle reached short sample limit (SSL) after only two quenches, compared with ∼100 when CTD-101K was used on a number of identical undulator coils [2]. TELENE's pot life of up to 3.5 h at 5 °C also ensures scalability to impregnate larger coil volumes. The undulator magnet with nine racetrack coils between 10 poles was wound at ANL. After the winding was complete, the magnet was assembled into its reaction tooling to be heat treated in argon at FNAL using well established treatment cycles [3]. It was then vacuum impregnated with pure TELENE at ANL, and later tested at FNAL in the SC R&D lab [4].

To further improve thermal stability and training in accelerator magnets, the idea of increasing superconductor's stability, usually based on its minimum quench energy (MQE), by inserting high specific heat (high-C_p) elements in SC wires dates back to the 1960s [5]. Then in the mid-2000s, a considerable improvement in stability to pulsed disturbances was obtained for NbTi windings, when distributing large heat capacity substances on the conductor during winding [6, 7]. The MQEs of the brushed coils were several times higher, and thermal efficiency was greatest for temperature diffusion times much smaller than the disturbance pulse duration. A few years ago, Hypertech and Bruker-OST have attempted to introduce high-C_p elements in their wire design [8]. More recently, Hypertech fabricated samples of a thin composite Cu/Gd_2O_3 tape, which can be inserted in Rutherford-type cables to increase the conductor C_p [9]. At NIMS and RIMTEC, TELENE was mixed with high-C_p ceramic powders such as Gd_2O_3, Gd_2O_2S and $HoCu_2$ [10]. The C_p temperature dependence was measured for TELENE mixed with $HoCu_2$, and the C_p temperature dependence as function of magnetic field was measured for TELENE mixed with Gd_2O_3, and Gd_2O_2S. NbTi SC wire samples impregnated with these resins were characterized and studied at FNAL by performing MQE measurements.

The radiation strength of insulating materials used in SC accelerator magnets is another key specification. The common limit of the Hi-Lumi LHC type magnets is 25 MGy of proton radiation for CTD-101K epoxy. In 2016 the resistance to Cobalt-60 gamma radiation was studied for DCP and epoxy resin bisphenol-A up to a dose of 3.3 MGy with a dose rate of 2 kGy h^{-1} [11]. By measuring and analyzing optical absorption, electrical conduction, dielectric and thermal properties, it was shown that the organic DCP resin had a superior gamma ray resistance with respect to the epoxy. For nonorganic materials, there is a dependence of material response on the type of beam irradiation. However, such a dependence is quite modest for organic materials, and the absorbed dose can be adequately used to qualify their radiation resistance. Therefore, resistance to gamma irradiation is a promising indicator to radiation strength and a Cobalt-60 gamma ray irradiation experiment is being run at an average dose rate of 8 kGy h^{-1} at the Takasaki Advanced Radiation Research Institute [12], which is part of the National Institutes for Quantum Science and Technology in Takasaki. Here we present results of mechanical properties of pure and mixed TELENE before and during irradiation up to about 10 MGy.

2. Experiment description

In this section, we will describe the experimental setups used for mixing the TELENE with high-C_p ceramic powders at NIMS (section 2.1); for measuring the resins' physical and mechanical properties at NIMS and KEK (section 2.2); for measuring the MQE of NbTi wire samples impregnated with the resins at FNAL (section 2.3); for fabricating and testing Nb_3Sn undulator short models impregnated with TELENE at ANL and FNAL (section 2.4); and for the Cobalt-60 gamma ray irradiation experiment at the Takasaki Advanced Radiation Research Institute (section 2.5).

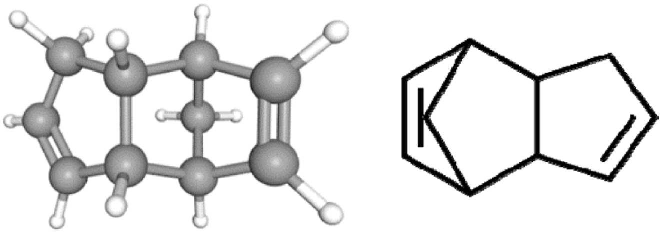

Figure 1. Molecular structure (left) and molecular formula (right) of TELENE®, i.e. $C_{10}H_{12}$.

Figure 2. Micrograph of the $HoCu_2$ particles produced by a standard melt and casting process.

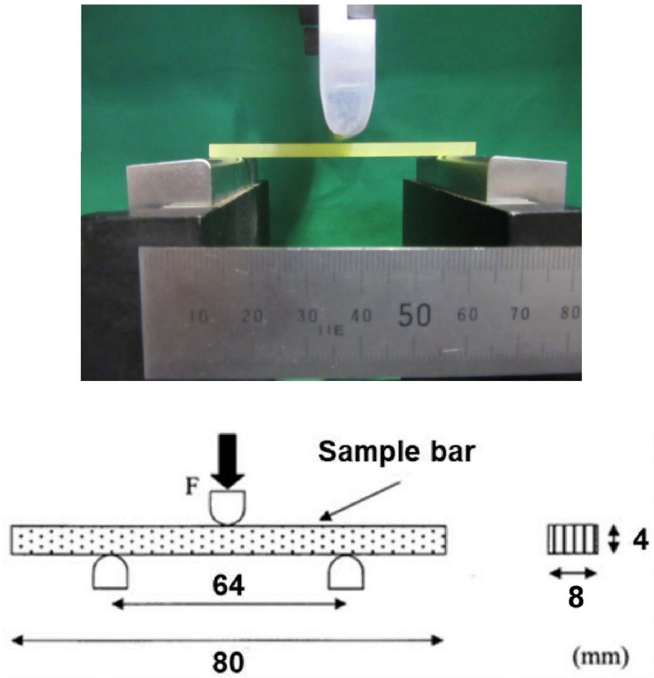

Figure 3. Picture (top) and schematic (bottom) of three-point bending test.

2.1. Fabrication of high-C_p resins and optimization of their composition

The high heat capacity resins are fabricated by combining a ceramics powder filler with TELENE using a planetary mixer. The TELENE is then mixed with a hardener or polymerization catalyst, which is a ruthenium complex, in 2/100 parts by wt. The curing time is controlled by the amount of phosphine derivatives as retardant. The viscosity of the resins is controlled by the volume fraction and average size of the powder filler. Therefore, the chemical composition, average powder size and volume fraction can be optimized. Using a Gd_2O_3 powder size of 0.7–1.2 μm, TELENE was mixed using three different concentrations, i.e. 45 wt%, 61 wt%, and 82 wt%. Using a Gd_2O_2S powder size of 10 μm, TELENE was mixed using seven different concentrations between 22 wt% to 87 wt%.

Because of its high-C_p and also smaller mass attenuation coefficient than Gd for thermal neutrons, in 2021 NIMS fabricated the first $HoCu_2$ powder by gas atomization, obtaining a particle size of 80 μm. A particle size of less than 30 μm was eventually achieved using a standard melt and casting process followed by a first stage grinding with a jaw crusher machine, and a second stage finer grinding with a planetary mill machine. The produced powder (figure 2) was used as a filler for TELENE with an 83 wt% concentration.

2.2. Measurements of physical and mechanical properties of each resin

Physical properties of the resins, such as viscosity, thermal conductivity, and specific heat C_p were measured at appropriate temperatures.

The viscosity was measured with a Brookfield-type viscometer, specifically an Eiko DV2T. Using a spindle speed of 60 rpm, a spindle of type LV-02 was used to measure viscosity values larger than 1 Pas, and one of type LV-04 to measure viscosity values lower than 1 Pas. The vscosity of TELENE was measured at 5 °C, 15 °C and 25 °C, and that of CTD-101K at 60 °C.

The C_p and thermal conductivity were measured with a DynaCool® physical property measurement system by Quantum Design. The C_p temperature dependence was measured for TELENE mixed with $HoCu_2$, and the C_p temperature dependence as function of magnetic field was measured for pure TELENE and TELENE mixed with Gd_2O_3, and Gd_2O_2S.

The mechanical properties that were measured for the resins include flexural modulus and flexural strength at room temperature. They were obtained through a three-point bending test, of which a picture and schematic are shown in figure 3. These tests follow ISO 178:2010-A1:2013. Sample size is 80 mm in length, 8 mm in width and 4 mm in thickness. The flexural tests were performed at room temperature with an Autograph AG-5000C tensile machine manufactured by Shimadzu. The flexural strength is the maximum stress in the stress vs. strain curve. The flexural modulus was obtained from the stress vs. strain curve between 0.05% strain and 0.25% strain.

2.3. Stability measurements of SC wire samples impregnated with high-C_p resins

Two sets of six 0.8 mm NbTi wire samples were prepared at FNAL and sent to NIMS for impregnation with TELENE only,

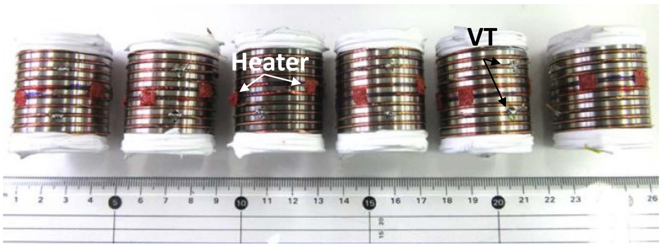

Figure 4. Picture of NbTi wire samples instrumented with two heaters each, and with the voltage taps (VT) attached before impregnation.

TELENE-82 wt%Gd_2O_3, and TELENE-87 wt%Gd_2O_2S resins. The MQE of impregnated wires is measured on ITER-type barrels. Two strain gauges of 4 mm and 1.5 mm length and width are used as 350 Ω heaters and glued to each sample using STYCAST 2850FT. The instrumentation wires are soldered before sample and strain gauges receive resin impregnation. Figure 4 shows a picture of NbTi wire samples instrumented with two heaters each, and with the voltage taps attached before impregnation.

A 200 W power supply provides the excitation voltage to the strain gauges. Using a LabView DAQ program, a pulse output is generated from the power supply and the voltage across the strain gauge is measured. With the I_c of the sample first measured, a constant bias current below I_c is applied to the sample and heat pulses are fired using the strain gauge. A separate quench protection system monitors the voltage across the sample and shuts down the power supply if the quench threshold is reached. By gradually increasing the pulse energy, the minimum energy that induces a quench is defined as the MQE of the sample [9]. In order to determine the most appropriate pulse duration range for each resin, the characteristic time, or thermal time constant τ, was calculated as $\tau = 4\ a^2/(\pi^2\ D)$, where $D = k/(\rho\ C_p)$ is the thermal diffusivity, k the thermal conductivity, ρ the material's density, and $2a$ the material's thickness. The thermal properties shown in table 1 were obtained by using $a = 1$ mm, ρ(STYCAST 2850 FT) = 2290 kg m^{-3}, ρ(TELENE) = 1030 kg m^{-3}, ρ(TELENE-82 wt%Gd_2O_3) = 3504 kg m^{-3}, and ρ(TELENE-87 wt%Gd_2O_2S) = 4110 kg m^{-3}. Based on the results for τ, the MQE was measured for heater pulse durations from 200 ms to 1.5 s.

2.4. Fabrication and test of Nb_3Sn undulator short model

In collaboration with FNAL and other labs, ANL developed a Nb_3Sn undulator to be installed in the Advanced Photon Source (APS) storage ring. Performance reproducibility close to 100% SSL was obtained by using several Nb_3Sn short models during the R&D phase. They were vacuum impregnated with CTD-101K, which is the same epoxy used for Nb_3Sn high field accelerator magnets. The same performance and reproducibility were later achieved on longer models. The training behavior of the undulator models was very similar to that of HEP accelerator magnets, requiring ∼100 quenches to approach SSL [2].

The design parameters of the undulator short model are detailed in table 2. These Nb_3Sn undulators with 18 mm period operate at a maximum magnetic field of about 5 T and maximum equivalent stress on the conductor below 100 MPa. To address instabilities at this field, a Restacked Rod Processed wire of 0.6 mm in diameter and with 144 SC subelements over 169 total subelements was used. Its equivalent subelement diameter is ∼35 μm, and the critical current density J_c (4.2 K, 12 T) is about 2500 A mm^{-2}. Each Nb_3Sn undulator short model has nine racetrack coils wound in a groove between 10 poles. There are 46 turns in each groove, and each period includes two grooves and two poles. The S2-glass braided Nb_3Sn wire is continuously wound turn-by-turn between the poles. A picture of a short undulator model is shown before impregnation in figure 5.

After winding, the magnet was assembled into an existing reaction tooling. The magnet model was heat treated at FNAL in argon atmosphere in a three-zone controlled tube furnace, using well-established treatment cycles [3]. Table 3 shows the nominal temperature values compared with the measured oven temperature. The temperature was averaged between two K-type calibrated and ungrounded thermocouples. Several witness samples of the same Nb_3Sn wire used in the coil were included in the furnace. Their critical current I_c was determined from measuring the V–I curve using an electrical field criterion of 0.1 μV cm^{-1}. The calculation of the expected coil SSL is obtained by intersecting the average I_c of these samples as function of the magnetic field with the magnet load line.

After winding and heat treatment, the magnet was vacuum impregnated with pure TELENE at ANL. The undulator was then tested at FNAL at 4.2 K in liquid helium at atmospheric pressure, in a cryostat of the SC R&D lab, by using an insert equipped with 2000 A DC leads. Figure 6 shows the TELENE impregnated magnet attached to the test insert. Two pairs of voltage taps, each covering half of the magnet, were used. The voltage tap wires were connected to an NI-9239 card of a compact RIO DAQ system. The NI card has four channels with an acquisition frequency of 50 kHz and 24 bits per channel. The threshold for the quench protection system was 100 mV for the differential voltage. When a quench is detected, the power supply is stopped, an insulated gate bipolar transistor switch opens and the current flows into a 0.125 Ω dump resistor, where the coil energy gets dissipated.

2.5. Gamma ray irradiation experiment

Gamma ray irradiation is being performed at the Takasaki Advanced Radiation Research Institute using a Cobalt-60 gamma irradiation facility. 40 samples (of 80 mm in length, 8 mm in width and 4 mm in thickness) each of pure TELENE, TELENE mixed with 82 wt%Gd_2O_3, with 87 wt%Gd_2O_2S, and with 83 wt%$HoCu_2$ are being irradiated in air atmosphere at an average absorbed dose rate of 8 kGy h^{-1}. Samples of CTD-101K epoxy were also included to verify the accuracy of the results. Each sample was 80 mm in length, 8 mm in width and 4 mm in thickness. Figure 7 shows the samples in their aluminum crate. The final goal for the entire irradiation campaign is to achieve 25 MGy+. Every month from start of irradiation

Table 1. Thermal properties of TELENE resins.

@4.2 K	ρ kg m^{-3}	k W (mK)$^{-1}$	C_p J (kg K)$^{-1}$	D m^2 s^{-1}	τ s
STYCAST 2850FT	2290	0.05	0.44	$500.0 \cdot 10^{-7}$	0.008
TELENE	1030	0.04	3.5	$111.0 \cdot 10^{-7}$	0.037
TELENE 82%Gd_2O_3	3504	0.02	20	$2.9 \cdot 10^{-7}$	1.420
TELENE 87%Gd_2O_2S	4110	0.09	60	$3.7 \cdot 10^{-7}$	1.111

Table 2. Undulator short model design parameters.

Design parameter	Value
No. periods	4.5
Groove width	5.5 mm
Groove depth	4.9 mm
Period length	18 mm
No. turns/groove	46
Nb_3Sn conductor	Ti-doped RRP
Conductor architecture	144/169
Conductor diameter	0.6 mm
Insulation material	S2-glass
Insulation thickness	65 μm
Final HT step	40 h at 650 °C

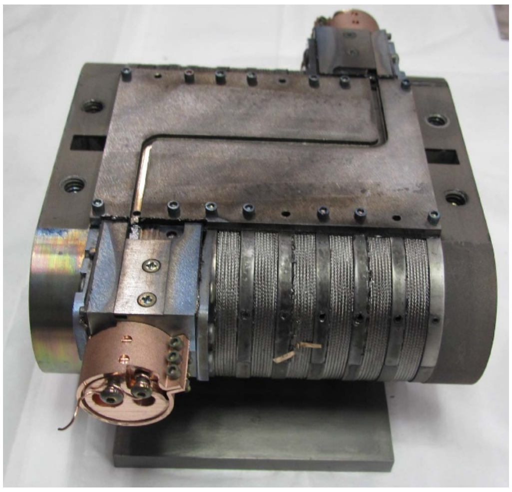

Figure 5. Picture of Nb_3Sn undulator short model after winding and reaction, and before impregnation.

Table 3. Nominal vs. obtained heat treatment cycle for undulator short model impregnated with TELENE.

Nominal		Obtained	
Time, h	T, °C	Time, h	T_{Ave}, °C
48	210	48	207
104	370	104	365
50	650	50	647

(i.e. every 2–3 MGy of absorbed dose), three samples of each resin were extracted from their aluminum rack and a htree-point bending test was performed at room temperature. Here we present results of mechanical properties of pure and mixed TELENE before and during irradiation up to about 10 MGy.

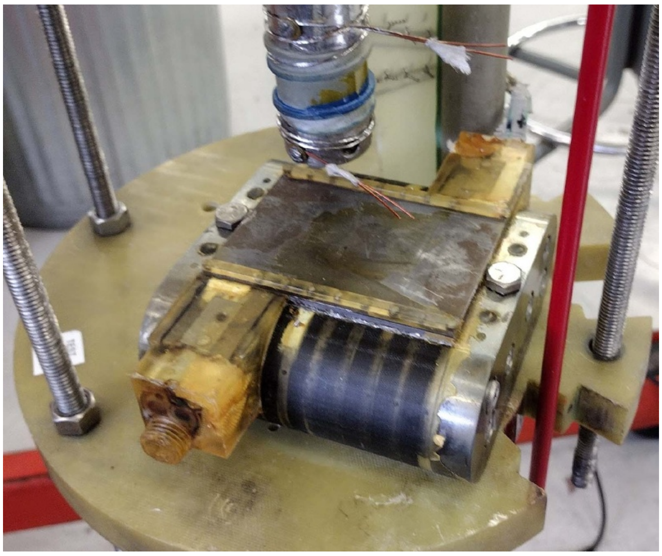

Figure 6. Picture of the first TELENE impregnated Nb_3Sn small undulator attached to its test insert.

Figure 7. Picture of aluminum crate containing the resins to be gamma ray irradiated in air atmosphere.

For nonorganic materials, there is a dependence of material response on the type of beam irradiation. However, such a dependence is modest for organic materials, and the absorbed dose can be used to qualify their radiation resistance. At a later stage, this could be confirmed with proton beam irradiation experiments at the BLIP facility at BNL.

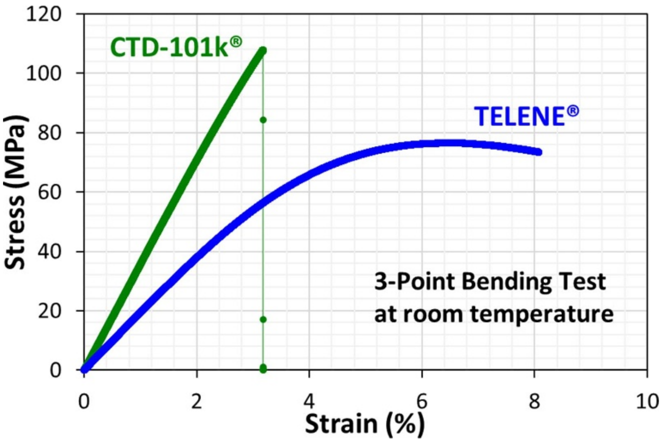

Figure 8. Comparison of flexural stress vs. strain curve between CTD-101K epoxy and TELENE resin at room temperature.

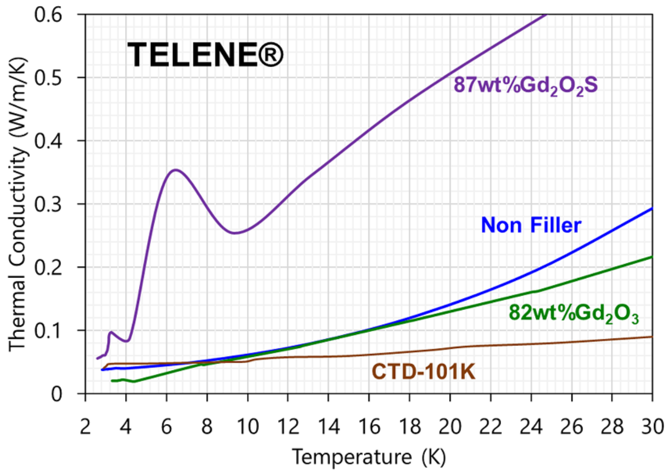

Figure 9. Thermal conductivity vs. temperature for CTD-101K epoxy, and for pure and mixed TELENE resins in absence of external magnetic field.

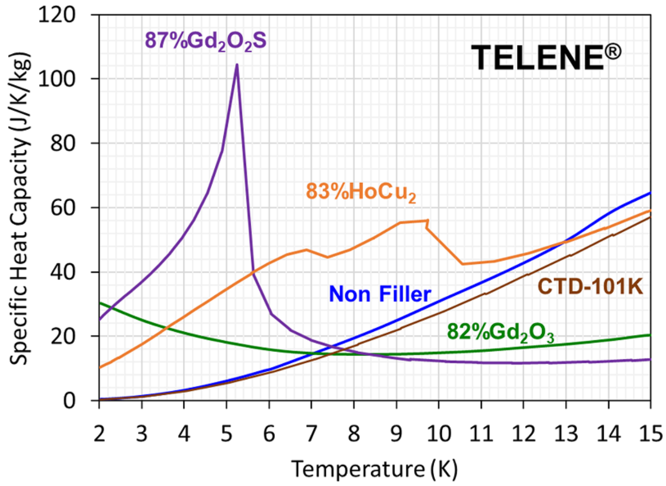

Figure 10. Specific heat vs. temperature for CTD-101K epoxy, and for pure and mixed TELENE resins in absence of external magnetic field.

3. Results and discussion

TELENE has close to 100% DCP composition. It was chosen for these studies because of the following main reasons: 1. Its ductility, i.e. the ability to accept large strains; 2. Its toughness, i.e. the amount of energy per unit volume that the material can absorb before rupturing, or the area underneath the stress vs. strain curve; 3. Its potential for radiation resistance. Figure 8 shows how much more ductile and tougher is pure TELENE with respect to CTD-101K epoxy at room temperature. TELENE preserves its ductility also at 77 K [13]. For adhesiveness to metals, inorganic materials and carbon fibers, polar functional groups were used in the TELENE curing agent.

The potential of improving TELENE's thermal properties by mixing it with high-C_p ceramic powders such as Gd_2O_3, Gd_2O_2S, and $HoCu_2$ was another component of this research.

In this section, we will present and discuss the results obtained for the resins' physical and mechanical properties (sections 3.1.1 and 3.1.2); for the MQE of NbTi wire samples impregnated with the resins (sections 3.2); for the TELENE impregnation and test of the first Nb_3Sn undulator short model, which includes impregnation process scalability (sections 3.3.1), magnet SSLs (sections 3.3.2), and magnet test results (sections 3.3.3); and for the Cobalt-60 gamma ray irradiation experiment up to 10 MGy at the Takasaki Advanced Radiation Research Institute (sections 3.4).

3.1. Measurements of physical and mechanical properties of each resin

3.1.1 Physical properties. Figures 9 and 10 show respectively the thermal conductivity k and specific heat C_p as function of temperature for CTD-101K epoxy, and for pure and mixed TELENE resins in absence of an external magnetic field. The specific heat as function of temperature at various external magnetic fields is shown in figure 11 for pure TELENE, in figure 12 for TELENE-45 wt%Gd_2O_3, and in figure 13 for TELENE-87 wt%Gd_2O_2S. The latter mixed resin has the largest thermal conductivity over the whole temperature range and a peak in C_p between 4.3 K and 5.3 K at fields between 0 and 8 T. Pure TELENE has a C_p which increases monotonically with temperature. Beyond 6 K, the C_p of pure TELENE is larger than that of TELENE mixed with Gd_2O_3 at any magnetic field.

3.1.2 Mechanical properties. The flexural stress vs. strain curves for pure and mixed TELENE resins are shown at room temperature in figure 14. After mixing the TELENE with hard ceramic particles, the material becomes stronger, i.e. larger flexural modulus, and less ductile. On the other hand, as seen in section 3.1.1, some of the TELENE mixed resins feature larger thermal conductivity and specific heat than pure TELENE. It is reasonable to speculate that TELENE's capability to absorb large strains and large energies be key to the undulator training performance as detailed in section 3.3. In the close future, these mechanical properties will be measured at 77 K in liquid

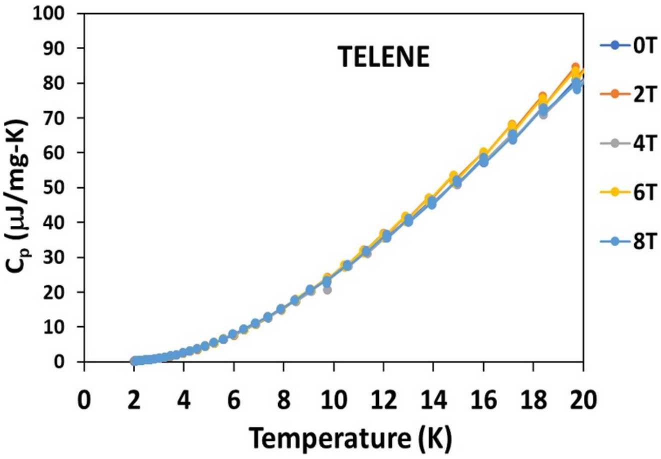

Figure 11. Specific heat C_p vs. temperature at various external magnetic fields for pure TELENE resin.

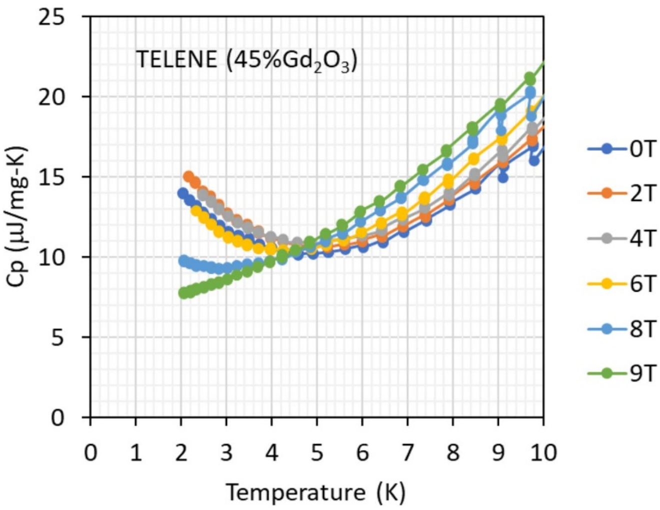

Figure 12. Specific heat C_p vs. temperature at various external magnetic fields for TELENE-45 wt%Gd_2O_3 mixed resin.

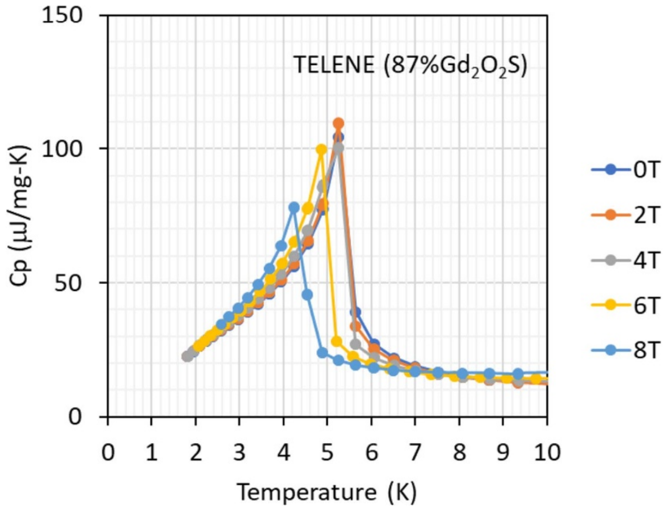

Figure 13. Specific heat C_p vs. temperature at various external magnetic fields for TELENE-87 wt%Gd_2O_2S mixed resin.

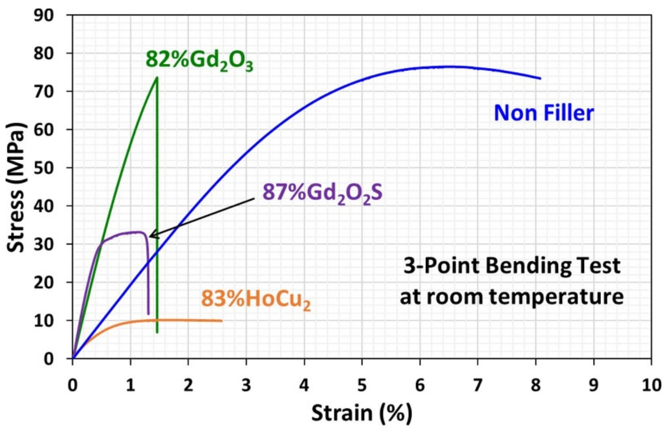

Figure 14. Flexural stress vs. strain curves for pure and mixed TELENE resins.

nitrogen. In a second part of this study, the impact on training behavior of the low diffusivity of the mixed resins with high-C_p has to be checked.

3.2. MQE measurements of NbTi wire samples impregnated with high-C_p resins

Based on the low diffusivity values obtained for the mixed TELENE resins shown in table 1, with a maximum time constant of 1.42 s for TELENE-82 wt%Gd_2O_3, the MQE of the impregnated 0.8 mm NbTi wire samples was measured for heater pulse durations from 200 ms to 1.5 s, with I_c% of up to 90% and magnetic fields between 6 and 9 T. At 9 T, the I_c (4.2 K) was 140 A. An example of results obtained at 9 T and at 80% of I_c is in figure 15. For pulse durations comparable to their time constant, both TELENE-82 wt%Gd_2O_3 and TELENE-87 wt%Gd_2O_sS show larger increases in MQE than pure TELENE.

3.3. Impregnation with TELENE and test of first Nb_3Sn undulator short model

After winding and heat treatment, the magnet was placed in a leak-tight impregnation mold for vacuum impregnation at ANL. The two-part resin, i.e. TELENE resin plus the polymerization catalyst, was mixed by weight. After injecting the resin, the assembly was cured at 120 °C for one hour. Due to the exothermic polymerization reaction, the internal temperature is higher by about 50 °C–100 °C, depending on the amount of resin.

As can be seen from figure 16, at room temperature the pot life of TELENE is 20 min. However, the viscosity of TELENE is much lower than that of epoxy, i.e. its consistency is like water.

3.3.1. Impregnation process scalability. As shown in figure 16, TELENE's pot life can be increased by lowering the temperature during the impregnation process, which is the

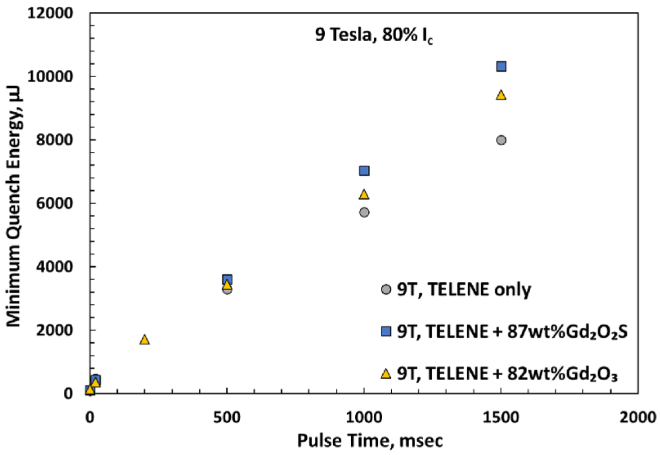

Figure 15. Minimum quench energy vs. heater pulse duration at 80% of the critical current I_c at 9 T for NbTi wire samples impregnated with pure and mixed TELENE.

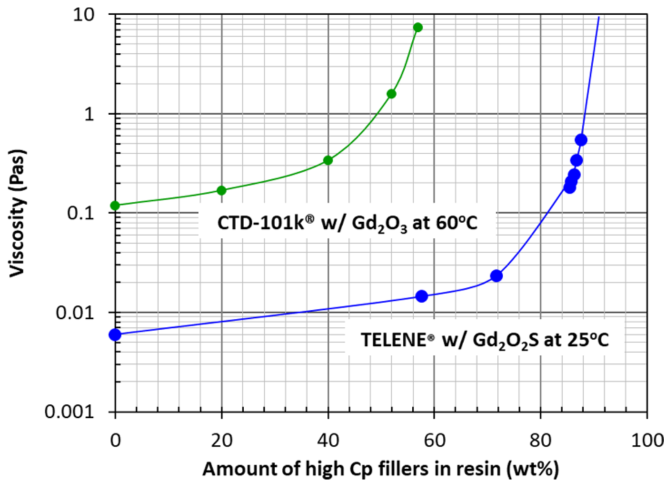

Figure 17. Viscosity as function of wt%Gd_2O_2S in TELENE at 25 °C compared with that at 60 °C of CTD-101K mixed with Gd_2O_3.

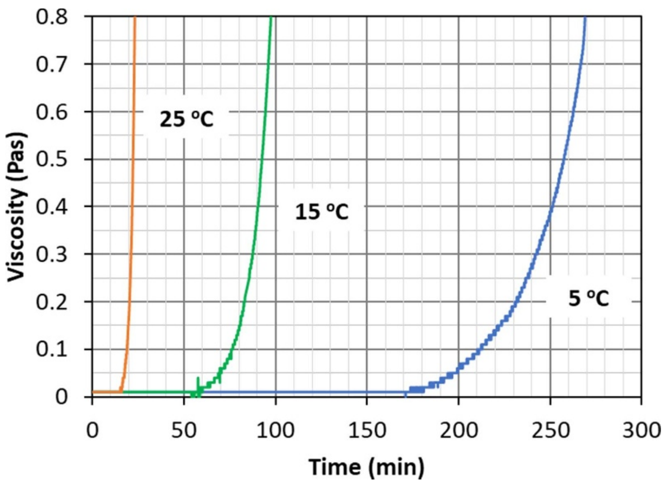

Figure 16. Viscosity as function of time for TELENE at different temperatures.

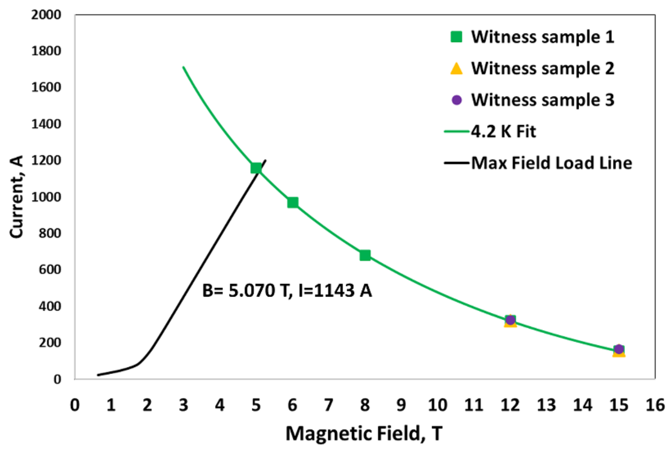

Figure 18. Short sample limit calculation of TELENE impregnated undulator model based on witness sample critical current test results.

Table 4. Pot life vs. temperature for pure TELENE.

Pot life, min	Temperature,° C
20	25
75	15
210	5

opposite of what is done for CTD-101K, for which the temperature is instead increased. The dependence of TELENE's pot life with temperature is shown also in table 4.

Scalability to larger impregnation volumes can be achieved by performing the impregnation process between 5 and 15 °C. Indeed, by using one epoxy inlet into tooling equipped with multiple vents and an inlet pressure of 2 bar, fill times with epoxy are less than 1.5 h for the HL-LHC IR quadrupoles that are 7.3 m long [14]. This includes about 45 min to inject CTD-101K in the coil's mold and fill it, and about 40 min for filling the outflow tank.

The viscosity of mixed TELENE resins is of the same order of magnitude as that of pure TELENE up to high fillers concentrations, as shown for instance at 25 °C for TELENE mixed with Gd_2O_2S in figure 17. On the other hand, the viscosity of CTD-101K is much more sensitive to the amount of high-C_p fillers, as shown for instance in figure 17 at 60 °C when mixed with Gd_2O_3. However, some particle sedimentation is expected to occur in TELENE mixed with high-C_p ceramic powders, due to the significant density difference. This factor will have to be accounted for when optimizing for the most effective mixed TELENE composition.

3.3.2. Magnet SSLs. The SSL for the first undulator short model was calculated based on the test results at 4.2 K of three Nb_3Sn witness samples that were included in the furnace with the coil. Figure 18 shows that the I_c vs. magnetic field curve for these samples intersects the maximum field load line of the undulator magnet at 1143 A and 5.07 T.

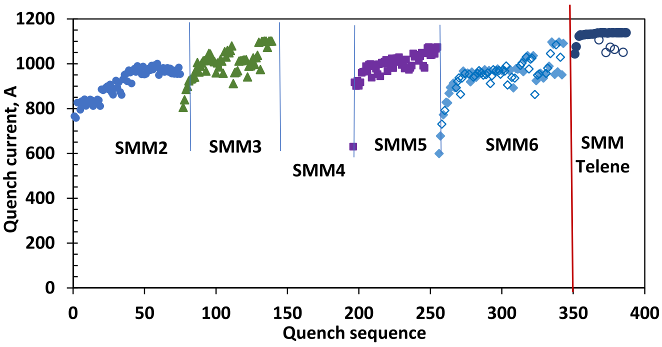

Figure 19. Quench history of TELENE impregnated short undulator model as compared with that of nearly identical undulator short models impregnated with CTD-101K. Data for Small Magnet Model 4, i.e. SMM4, are not shown because it was damaged.

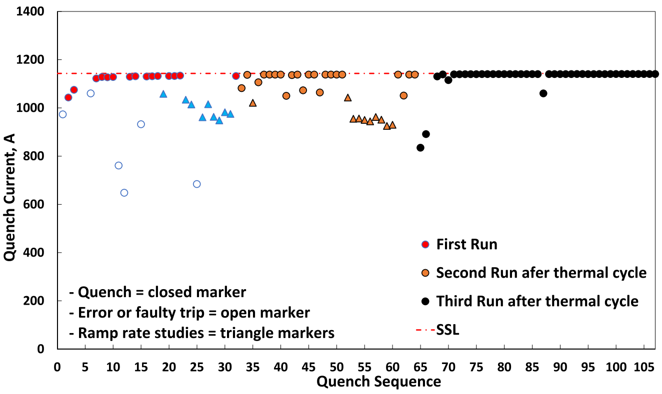

Figure 20. Quench history, including two thermal cycles, for TELENE impregnated short undulator model. Actual quenches at the standard ramp rate of 1 A s^{-1} are indicated with closed circles. The maximum achieved current was 1140 A, or 99.7% SSL.

3.3.3. Magnet test results. The quench data for the first TELENE impregnated short undulator model as compared with identical undulator short models impregnated with CTD-101K are shown in figure 19. Data for Small Magnet Model 4, i.e. SMM4, are not shown because it was damaged. Figure 20 shows in more detail the quench history of this first undulator model, including two thermal cycles. Actual quenches obtained at the standard ramp rate of 1 A s^{-1} are indicated with closed circles. Closed triangles indicate quenches produced during ramp rate studies, which were performed up to ramp rates of 50 A s^{-1}. Open circles represent faulty trips due to overflow of the DAQ buffer's memory that spuriously activated the quench protection feature, and stopped the data taking. This problem was subsequently fixed before proceeding with the second and third runs, where no faulty trips appeared anymore.

As can be seen, the first quench at 1043 A occurred at about 91% of SSL, which was 1143 A. It took only two quenches before achieving SSL, compared to ∼100 quenches needed to reach a plateau for the nearly identical undulator coils impregnated with CTD-101K [2].

The quench results during the first and second thermal cycles, i.e. second and third test sequences performed after warming up the magnet to room temperature and cooling it down again, are also shown in figure 20. In this second and third runs, the SSL was reached once again in no more than two quenches. However, these sequences also showed a number of current drops, down to 92%–97% of SSL. The analysis of the voltage tap signals did not provide any insight on the nature of these quenches, and additional instrumentation will be needed to investigate this phenomenon.

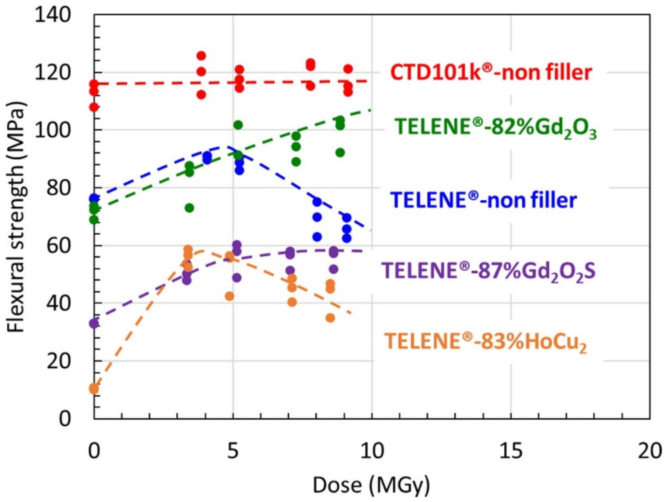

Figure 21. Flexural strength as function of Co-60 Gamma ray dose for pure and mixed TELENE compared with CTD-101K.

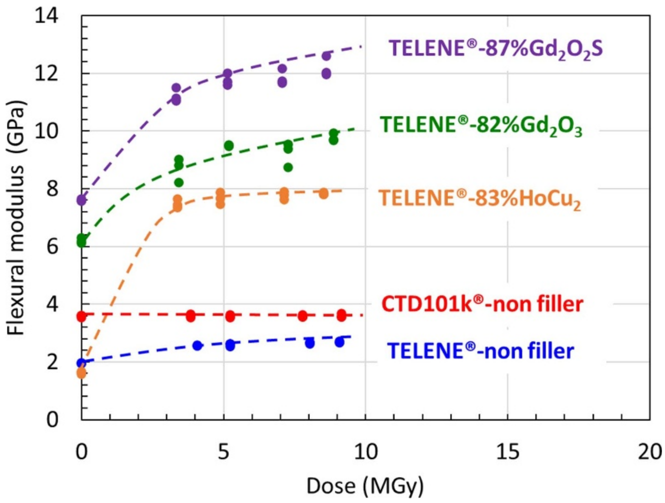

Figure 22. Flexural modulus as function of Co-60 Gamma ray dose for pure and mixed TELENE compared with CTD-101K.

3.4. Cobalt-60 gamma ray irradiation experiment up to 10 MGy

Figures 21 and 22 show the flexural strength and the flexural modulus respectively as function of Gamma ray dose for pure and mixed TELENE compared with CTD-101K. The flexural modulus monotonically increased by about 40% for pure TELENE, more than 60% for TELENE-82 wt%Gd_2O_3 and

TELENE-87 wt%Gd_2O_2S, and more than 450% for TELENE-83 wt%$HoCu_2$. The flexural strength monotonically increased for TELENE-82 wt%Gd_2O_3 and TELENE-87 wt%Gd_2O_2S.

4. Conclusions

By replacing CTD-101K with TELENE to impregnate a short ANL Nb_3Sn undulator coil, training and magnet retraining were nearly eliminated before reaching SSL at over 1100 A, which is much larger than the 450 A nominal current of the NbTi undulators operating in the ANL APS. TELENE will enable operation of Nb_3Sn undulators much closer to their SSL, expanding the energy range and brightness intensity of light sources. Pure TELENE is Co-60 gamma radiation resistant up to 7–8 MGy, and therefore already applicable for impregnation of insertion devices for synchrotron light sources, operating in lower radiation environments than high energy colliders.

TELENE-82 wt%Gd_2O_3 and TELENE-87 wt%Gd_2O_2S have proven to be exceptionally radiation resistant to Co-60 gamma irradiation. When combined with the ductility and toughness properties of TELENE, these resins are expected to show superior training performance with respect to CTD-101K. Impregnating an undulator coil with TELENE mixed with Gd_2O_2S powder will verify whether the coil stability further improves, or whether its low diffusivity will require engineering the material with high-thermal conductivity components.

TELENE was successful to prevent training in the Nb_3Sn ANL undulator, which produces a maximum magnetic field of about 5 T and maximum equivalent stress on the conductor of less than 100 MPa. The next necessary step is to check whether the developed resins can lead also to a reduction in training in stress managed magnets, which is the current core design in the US Magnet Development Program.

By successfully reducing coil training, and based on the current radiation resistance results, TELENE impregnation technology is expected to have direct application to high field Nb_3Sn dipole and quadrupole magnets for high radiation environments. Short magnet training will lead to better magnet reliability, lower magnet margins, lower risk and substantial saving in accelerators' commissioning costs.

Data availability statement

All data that support the findings of this study are included within the article (and any supplementary files).

ORCID iDs

Emanuela Barzi https://orcid.org/0000-0001-5829-2147
Akihiro Kikuchi https://orcid.org/0000-0002-5044-7156

References

[1] U.S. Department of Energy, Office of Science 2020 The 2020 Updated Roadmaps for the U.S. Magnet Development Program (arXiv:2011.09539)
[2] Kesgin I *et al* 2019 Development of short-period Nb_3Sn superconducting planar undulator *IEEE Trans. Appl. Supercond.* **29** 4100504
[3] Barzi E, Turrioni D, Ivanyushenkov Y, Kasa M, Kesgin I and Zlobin I A V 2020 Heat treatment studies of Nb_3Sn RRP wires for superconducting planar undulators *IEEE Trans. Appl. Supercond.* **30** 6001005
[4] Barzi E, Andreev N, Apollinari G, Bucciarelli F, Lombardo V, Nobrega F, Turrioni D, Yamada R and Zlobin A V 2013 Superconducting strand and cable development for the LHC upgrades and beyond *IEEE Trans. Appl. Supercond.* **23** 6001112
[5] Hancox R 1968 Enthalpy stabilized superconducting magnets *IEEE Trans. Magn.* **4** 486–8
[6] Alekseev P, Boev A, Keilin V, Kovalev I, Kruglov S, Lazukov V and Sadikov I 2004 Experimental evidence of considerable stability increase in superconducting windings with extremely high specific heat substances *Cryogenics* **44** 763–6
[7] Alekseev P, Boev A, Keilin V, Kovalev I, Kozub S, Kostrov E, Kruglov S, Lazukov V, Sadikov I and Shutova D 2006 Influence of high heat capacity substances doping on quench currents of fast amped superconducting oval windings *Cryogenics* **46** 252–5
[8] Xu X, Li P, Zlobin A V and Peng X 2018 Improvement of stability of Nb_3Sn superconductors by introducing high specific heat substances *Supercond. Sci. Technol.* **31** 03LT02
[9] Barzi E, Novitsky I, Rusy A, Turrioni D, Zlobin A V, Peng X and Tomsic M 2021 Test of superconducting wires and rutherford cables with high specific heat *IEEE Trans. Appl. Supercond.* **31** 9404812
[10] Kikuchi A and Takeychi M Patent pending
[11] Miyamoto M, Tomite N and Ohki Y 2016 Comparison of gamma-ray resistance between dicyclopentadiene resin and epoxy resin *IEEE Trans. Dielectr. Electr. Insul.* **23** 2270
[12] Musso A, Nakamoto T, Grande B D, Borderas C L, da Sousa D F, Sugano M, Ogitsu T and Tavares S S 2022 Characterization of the raidation resistance of glass fiber reinforced plastics for superconducting magnets *IEEE Trans. Appl. Supercond.* **32** 7700405
[13] RIMTEC corporation (available at: www.rimtec.co.jp/en/technology/behavior.html)
[14] Axensalva J and Nobrega F 2023 private communication